Cell Proliferation

Cell Prolif., 2015, **48**, 561–572 doi: 10.1111/cpr.12203

Ataxia-telangiectasia mutated (ATM) participates in the regulation of ionizing radiation-induced cell death *via* MAPK14 in lung cancer H1299 cells

Nan Liang*,†, Rui Zhong*, Xue Hou‡, Gang Zhao*, Shumei Ma*,§, Guanghui Cheng¶ and Xiaodong Liu*,‡

**Key Laboratory of Radiobiology (Ministry of Health), School of Public Health, Jilin University, Changchun 130021, China, †University of Manitoba, Winnipeg, Manitoba R3E 0V9, Canada, ‡Department of Radiation Oncology, 1st Hospital Affiliated to Jilin University, Changchun 130021, China, §University of Manitoba, Manitoba Institute of Cell Biology, Winnipeg, Manitoba R3E 0V9, Canada and ¶Department of Radiation Oncology, China-Japan Union Hospital of Jilin University, Changchun 130021, China*

Received 28 April 2015; revision accepted 20 June 2015

Abstract

Objectives: The role of Ataxia-telangiectasia mutated (ATM) in response to DNA damage has previously been studied, but its underlying mechanisms specific to ionizing radiation (IR) have remained to be elucidated. In this study, function of ATM on radiation-induced cell death in lung cancer H1299 cells was analysed.

Materials and methods: Human lung cancer cells, H1299, were used, and cell models with $ATM^{-/-}$ and $MAPK14^{-/-}$ were established by genetic engineering. Radiosensitivity was analysed using colony formation assays. Western blotting and co-immunoprecipitation were implemented to detect protein expression and interaction. MDC staining and GFP-LC3 relocalization were used to detect autophagy.

Results: Autophagy as well as phosphorylation of ATM was activated by ionizing radiation. Both the inhibitor of ATM, KU55933 and ATM silencing reduced phosphorylation of ATM and MAPKAPK2 expression. Both $ATM^{-/-}$ and $MAPK14^{-/-}$ cells displayed hypersensitivity. IR increased autophagy level by more than 129% in DMSO-treated cells, while only by 47% and 27% in KU55933-treated and $ATM^{-/-}$ cells respectively. MAPK14 knock-down alone gave rise to the basal autophagy level, but decreased notably after IR. KU55933 and ATM knock-down inhibited IR-induced autophagy by activating mTOR pathways. Both Beclin1–PI3KIII and Beclin1–MAPKAPK2 interactions as were remarkably affected by silencing either ATM or MAPK14.

Conclusions: ATM promoted IR-induced autophagy *via* the MAPK14 pathway, mTOR pathway and Beclin1/PI3KIII complexes. MAPK14 contributed to radiosensitization of H1299 cells.

Correspondence: Xiaodong Liu, 1163 Xinmin Street, Changchun, Jilin 130021, China. Tel.: 86 431 85619418; Fax: +86 431 85619418; E-mail: liuxd2014@126.com and Guanghui Cheng, 126 Xiantai Street, Changchun, Jilin 130033, China. Tel.: +86 431 85619418; Fax: +86 431 85619418; E-mail: 827229953@qq.com

Introduction

Radiotherapy plays a major role in treatment of non-small cell lung cancer (NSCLC) (1). It has been estimated that as many as 61% of all lung cancer patients receive radiotherapy (RT) as part of their first-line treatment (2). As is known, efficacy of radiotherapy is determined by radiation-induced cell death which includes programmed cell death (PCD) and non-programmed cell death. PCD consists of type I (apoptosis), type II (autophagic cell death). In our previous studies, emphasis has been laid mostly on mechanisms of autophagy and the molecular switch between autophagy and apoptosis.

Autophagy is an evolutionarily conserved intracellular self-catabolic process for maintaining cell homoeostasis by turnover of cellular components. It functions as an endogenous clearing system safeguarding cell integrity, by degrading and recycling long-lived proteins, and damaged organelles (such as endoplasmic reticulum, Golgi apparatus and mitochondria) by lysosomal/vacuolar processes (3). Autophagy can be triggered by diverse stimuli, such as starvation, reactive oxygen species (ROS), pathogens, hypoxia and ionizing radiation (IR) (4–8), and it has been reported to be an important mechanism, especially in development of cancer (9,10). Autophagy can either play a pro-survival role and deteriorate the cancer therapeutic outcome, or

work as programmed cell death to ameliorate overall anti-tumour efficacy (11), depending on cellular context, strength and duration of stress-inducing signals (12–14).

ATM (Ataxia-telangiectasia mutated) is a serine/threonine protein kinase and a member of the phosphoinositide 3-kinase-related protein kinase (PIKK) family. The consensus of the ATM phosphorylation motif is hydrophobic-X-hydrophobic-[S/T]-Q. The most important role of ATM is to be the first responder to DNA double strand breaks (DSBs), and to phosphorylate downstream substrates involved in DNA repair and cell cycle regulation. Interestingly, ATM has recently been shown to regulate autophagy in response to genotoxic and oxidative stimulation (15–20). However, functions of ATM in IR-induced cell death and the underlying mechanisms have remained to be elucidated.

Recently, MAPK14 (mitogen-activated protein kinase 14) has been reported to share a phosphorylation site with ATM/ATR, at TQ 263, after DNA damage by IR (21). MAPK14 (also called p38 MAPK), plays an important role in numerous processes including survival, differentiation and cell proliferation (22,23). According to many reports, MAPK14 has a dual role in autophagy, both as positive and negative regulator. On the one hand, prolonged inactivation of MAPK14 triggers AMPK-dependent nuclear localization of FoxO3A and subsequent activation of its target genes, consequently leading to autophagy (24–27). On the other hand, activation of MAPK14 induces autophagy by transcriptional regulation of autophagy-related genes (28–30). However up to now, whether or not MAPK14 is the substrate of ATM, and its specific role in IR-induced cell death, has not been exactly clarified.

In our previous work (31), we found that ATM played an important role in ionizing radiation-induced autophagy in human cervical cancer Hela cells, and MAPK14 might possibly be downstream of ATM. To explore whether this mechanism was universal in other cancers and to further identify this pathway, we continued to validate functions and relationships of ATM and MAPK14, in human lung cancer H1299 cells, more attention being paid to MAPKAPK2, directly downstream of MAPK14. The majority of the changes were highly consistent with our previous hypothesis, except for the effect of MAPK14 silencing itself on autophagy, which might result from partial deletion of p53 in H1299 cells. This article is an extension of previous published studies and provides further solid evidence of our hypotheses. This helps understanding ATM-mediated cell death in further detail and might possibly provide a basis for novel therapy in future cancer care.

Materials and methods

Cell lines, antibodies and reagents

H1299 cells (human lung cancer cell line, lacking expression of p53 protein) were cultured in RPMI 1640 medium (GIBCO) supplemented with 10% foetal bovine serum (FBS) and 1% penicillin–streptomycin (Invitrogen, Carlsbad, CA, USA) in glass Petri dishes at 37 °C in a 5% CO_2 incubator.

Foetal bovine serum (FBS), Cell Counting Kit-8 (CCK-8; Dojin Laboratories, Kumamoto, Japan) and monodansylcadaverine (MDC) were purchased from Sigma Chemical (St. Louis, MO, USA), and pSUPER retroviral vector was obtained from OligoEngine (Seattle, WA, USA). Antibodies of MAPLC3, ATM, p-ATM, PI3KIII, mTOR, p-mTOR, P70S6K and p-P70S6K were purchased from Cell Signaling. Anti-MAPK14, anti-p53, anti-AKT, anti-Beclin 1 and anti-GAPDH (glyceraldehyde 3-phosphate dehydrogenase) were obtained from Santa Cruz Biotechnology (Santa Cruz, CA, USA). Peroxidase-conjugated anti-mouse IgG and peroxidase-conjugated anti-rabbit IgG were purchased at Santa Cruz Biotechnology. KU55933 was obtained from Calbiochem-EMD Biosciences, Inc (La Jolla, CA, USA).

shRNA construct and transfection

shRNAs were designed according to "www.idtdna.com" and were synthesized, denatured, annealed and ligated to Psuper vector at BglII and HindIII sites; sequences are as follows: for ATM, sense sequence: 5′-GATCTGCCAGA CAGCCGTGACTTATTCAAGAGATAAGTCACGGC TGTCTGGCTTTTTA-3′; antisense sequence: 5′-AGCT TAAAAAGCCAGACAGCCGTGACTTATCTCTTGAA TAAGTCACGGCTGTCTGGCA-3′; for MAPK14: sense sequence: 5′-GATCTGGCAGATCTGAACAACATTTT CAAGAGAAATGTTGTTCAGATCTGCCTTTTTA-3′; antisense sequence: 5′-AGCTTAAAAAGGCAGATCT GAACAACATTTCTCTTGAAAATGTTGTTCAGATC TGCCA-3′. A control construct expressing a scrambled sequence with no significant homology to any known mammalian mRNAs was used as shRNA control, pSUPER. All plasmids were constructed in our laboratory. Plasmids were transfected into 293 T packaging cells by calcium phosphate co-precipitation, to produce pseudovirus particles [(Ampho Pack plasmid 10 μg, Psuper-shRNA plasmid 10 μg, 2 mol/LCaCl2 31 μl, ddH2O to 250 μl, and 2 × HEPES buffer salt solution (HBS) 250 μl)]. Supernatant containing pseudovirus particles was collected after 72 h and then used to infect H1299 cells together with polybrene (8 μg/ml). Positive stable

cell clones were selected by growing cells with puromycin (0.8 μg/ml) for 1 week.

Radiation

X-ray generation (X-RAD 320ix; Precision X-ray Inc., North Branford, CT, USA) was utilized to deliver radiation at 0.40 Gy/min.

Western blot analysis

Total proteins were extracted using RIPA lysis buffer [HEPES(50 mM), NaCl (150 m, EDTA(1 mM), EGTA (2.5 mM), NaF(10 mM, DTT(1 mM), SV(1 mM), PMSF (1 mM), NP-40(1%), SDS(0.1%)], and 2 ml aliquots were mixed with 20 μl protease inhibitor cocktail and the lysates was laid on ice for 5 min, followed by sonication. Supernatant was removed to a further tube after centrifuging at 12 000 rpm for 10 min and lysate was mixed with 5× SDS loading buffer (BioTeke, Beijing, China) and heated to 95 °C for 5 min. Of total protein, 40 μg was separated by SDS-PAGE, and transferred to nitrocellulose membranes ehich were then blocked in 5% non-fat dried milk in Tris-buffered saline (TBS) and Tween 20 (10 mmol/l Tris, pH 7.5, 100 mmol/l NaCl and 0.1% Tween 20) at room temperature for 1.5 h, incubated with appropriate primary antibody overnight at 4 °C, and horseradish peroxidase-conjugated secondary antibodies at room temperature for 1 h. Finally, signals were visualized by using Pierce chemiluminescence detection system according to the manufacturer's instruction (Santa Cruz Biotechnology); GAPDH protein was used as loading control. Intensity of protein bands was quantified using image software (Quantity One) and ratios of specific bands to loading control were analysed.

Co-immunoprecipitation

H1299 cells were washed twice in cold phosphate-buffered saline (PBS), then lysed using 1 ml radioimmunoprecipitation (RIPA) buffer (50 mM Tris-HCl [pH 6.8], 0.1% SDS, 150 mM NaCl, 1 mM EDTA, 0.1 mM Na_3VO_4, 1 mM sodium fluoride [NaF], 1% Triton X-100, 1% NP40, 1 mM dithiothreitol, and 1 mM PMSF, 1 mg/ml aprotinin, 1 mg/ml leupeptin, 1 mg/ml pepstatin A). After 60 min lysis on ice and centrifugation at 12,000 rpm for 15 min, supernatants were collected. Of total protein, 1 mg was incubated overnight with 20 μl aliquot of protein A-Sepharose CL-4B (GE, Uppsala, Sweden) beads and then immunoprecipitated with Beclin1 antibody. Samples were then washed five times in 500 μl lysing buffer, eluted in 40 μl loading buffer and boiled for 5 min. Eluted proteins were analysed by western blotting.

Colony formation assay

For colony formation assays, cells were seeded into six-well plates in triplicate and then incubated in standard RPMI 1640 culture medium for 24 h. Different doses of radiation (0, 2, 4, 6, 8 Gy) were given. Two weeks later, the cells were fixed in 100% formaldehyde and stained with 0.5% crystal violet. Surviving colonies of >50 cells were scored by viewing with a dissection microscope (Olympus XSZ-D2, Tokyo, Japan). The surviving fraction for a given treatment dose was calculated as

$$\mathrm{SF}(\%) = (\mathrm{Sx}/\mathrm{S0}) \times 100\%,$$

where Sx and S0 represented irradiated samples and sham-irradiated ones respectively. The dose–survival curve for each experiment was constructed by plotting surviving fractions against dose, in semilogarithmic plots. The multi-target single-hit model Origin 8.0 was applied to fit cell survival fraction curves, $S = 1 - (1 - e^{-D/D0})^N$, and then mean lethal dose (D0) was calculated.

CCK-8 assay for detection of cell viability

H1299 cells were seeded in 96-well plates at 4000 cells/well, followed by KU55933 with indicated concentrations; DMSO was used as control. Forty-eight hours after different treatments, 10 μl CCK-8 solution was added to each well and cells were incubated for 2 h. Absorbance was measured at 450 nm using a microplate reader (Synergy HT, Bio-Tek, Winooski, VT, USA).

GFP-LC3 relocalization assay

pQN-GFP-LC3 plasmid was transfected into packaging cells 293 T, by calcium phosphate co-precipitation, to produce pseudovirus particles [(Ampho Pack plasmid 10 μg, pQN-GFP-LC3 10 μg, 2 mol/LCaCl2 31 μl, ddH2O to 250 μl and 2 × HEPES buffer salt solution (HBS) 250 μl)]. Pseudovirus supernatant was collected after 72 h and then used to infect H1299 cells together with polybrene (8 μg/ml). Positive stable cell clones were selected by growing cells with G418 (800 μg/ml) for 2 weeks. H1299 cells stably expressing GFP-LC3 were plated (1×10^5) in six-well plates on glass coverslips and exposed to indicated doses of IR. After 24 h they were fixed in methanol for 10 min. GFP-LC3 puncta were visualized using an inverted fluorescence microscope equipped with CCD cameras (Olympus XSZ-D2). Images were captured and analysed for

presence of more than five punctae per cell. Data are represented as puncta-positive cells normalized to total number of GFP-positive cells.

MDC staining assay

H1299 cells were seeded on coverslips and incubated overnight. Twenty-four hours after indicated irradiation treatment, they were washed twice in cold phosphate-buffered saline (PBS). Autophagic vacuoles were labelled with monodansylcadaverine (MDC) by incubating cells in 50 mμ MDC in 1640 medium at 37 °C for 1 h. They were then washed three times in PBS and fixed in a solution of 4% paraformaldehyde, for 15 min. Flow cytometry was used to detect fluorescence developed.

Assay of apoptosis

H1299 cells were plated in six-well plates and treated with indicated doses of IR. Twenty-four hours later, they were collected and washed three times in PBS followed by staining with Annexin V-FITC Apoptosis Detection Kit I (BD Biosciences, San Diego, CA, USA) according to the manufacturer's recommendation. The cells were then detected by flow cytometry (BD FACS Canto) and analysed using FCS Express v2.0 software.

Statistical analysis

Statistical evaluations were presented as mean ± SD. Data were analysed using the Student's *t*-test, one-way ANOVA test or χ^2 test using SPSS v17.10 software (SPSS Statistics for Windows, Version 17.0. Chicago: SPSS Inc, USA) for statistical significance. $P < 0.05$ was considered significant.

Results

IR induced autophagy and ATM phosphorylation in H1299 cells

H1299 cells were exposed to different doses of radiation, and MAPLC3 was detected as the specific marker of autophagy. Appearance of punctuated cytosolic MAPLC3 and conversion of MAPLC3-I to MAPLC3-II indicated involvement of MAPLC3 in autophagosome formation. Western blotting revealed MAPLC3-II/MAPLC3-I ratio increased in a dose-dependent manner (Fig. 1a,b). Autophagy was also determined using monodansylcadaverine (MDC) staining, and increase in MDC-positive cells illustrated occurrence of autophagy after IR (Fig. 1c). H1299 cells transfected with GFP-LC3 exhibited obvious increase in punctate cytoplasmic structures (autophagic vesicles) after IR treatment, compared to the mock-irradiation group (Fig. 1c). As expected, exposure of H1299 cells to IR induced ATM phosphorylation at Ser 1981 (Fig. 1d,e). Peak level P-ATM was detected 1 h after IR, which decreased to baseline at 4 h compared to mock-irradiation group. Taken together, IR induced both autophagy and ATM phosphorylation, suggesting that ATM might participate in regulation of autophagy in H1299 cells.

Inhibition of ATM reduced expression of MAPK14 and phosphorylation of MAPKAPK2

To study specific functions of ATM, inhibitor of ATM kinase, KU55933, was used. Expression of phosphorylated ATM was inhibited by 700 nmol/l of KU55933 without killing any cells (Fig. S1). Meanwhile, phosphorylation of MAPKAPK2, directly downstream of MAPK14, also reduced significantly after KU55933 treatment (Fig. 2a). $ATM^{-/-}$ and $MAPK14^{-/-}$ cell models were then established. As shown in (Fig. 2b), silencing of MAPK14 had no effect on ATM expression, but silencing of ATM reduced expression of MAPK14 significantly, suggesting that MAPK14 might be one of the substrates of ATM and could be regulated by it.

Loss of ATM or MAPK14 resulted in hypersensitivity to IR while having no effect on apoptosis

Aiming to elucidate functions of ATM and MAPK14 in DNA damage, radiosensitivity was detected. As shown in Fig. 2c and 2d, colony formation assays demonstrated that $ATM^{-/-}$ cells and $MAPK14^{-/-}$ cells had lower D0 values, 1.44 and 1.52 respectively, compared to 2.07 in Psuper (vector control) cells. Likewise, treatment with KU55933 also led to lower D0 value compared to DMSO-treated cells (1.59 versus 2.21). These results indicate that cells lacking ATM or MAPK14 were hypersensitive in response to DNA damage induced by IR.

To discover the major killing mechanism of IR, cancer cell to die, apoptosis was then detected. Percentages of apoptotic cells increased from 8.17% to 11.99% before and after IR in DMSO-treated cells and from 6.43% to 12.06% in KU55933-treated cells respectively. There was no significant difference between cells treated with KU55933 or without the treatment [5.63% (12.06–6.43%) versus 3.82% (11.99–8.17%)]. Simultaneously, percentages of apoptotic cells increased by 3.30%, 5.97% and 4.28% in Psuper cells, $ATM^{-/-}$ cells and $MAPK14^{-/-}$ cells respectively. No significant change in IR-induced apoptosis was observed in wild type and

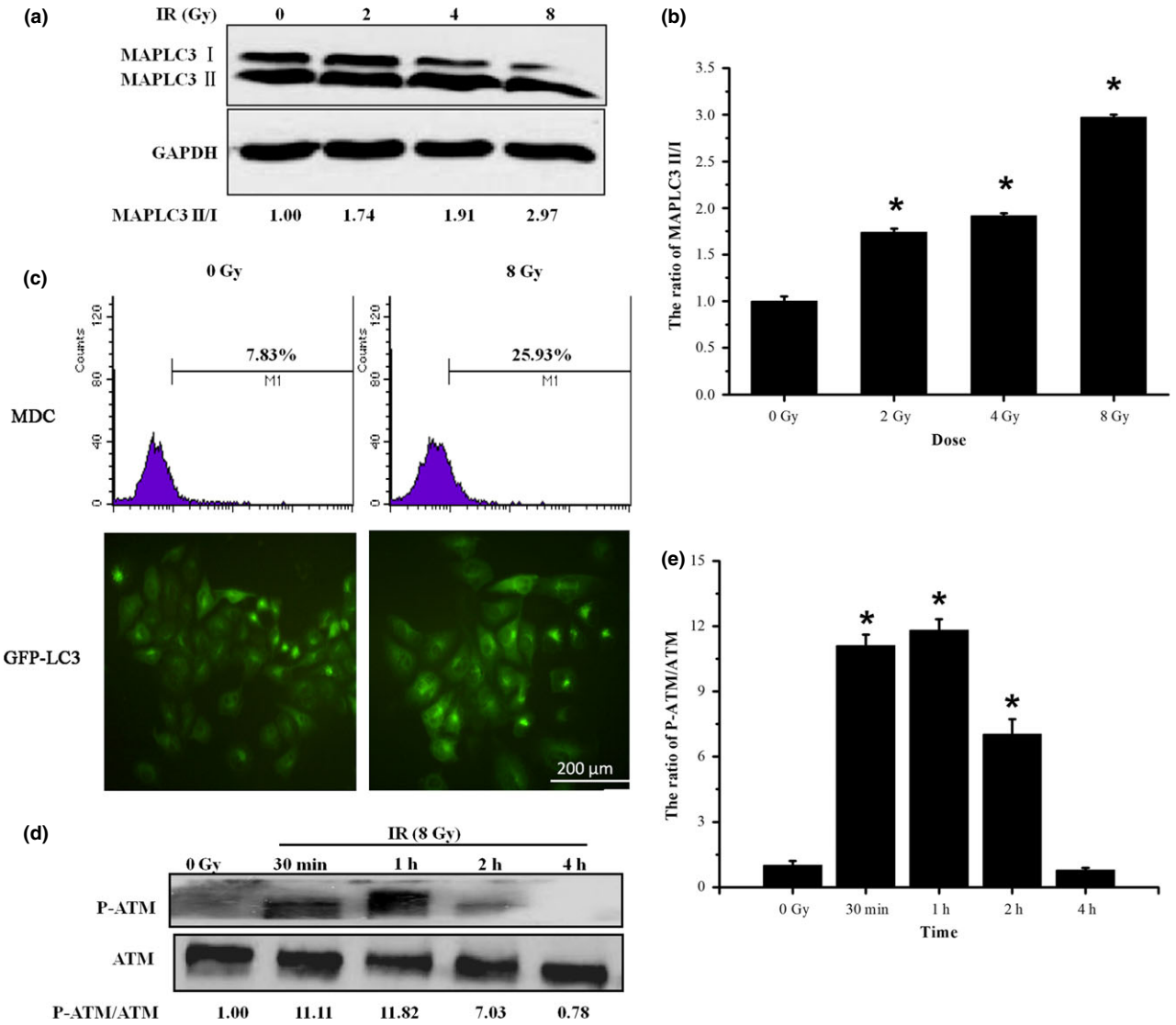

Figure 1. IR induced autophagy and phosphorylation of ATM in H1299 cells. (a and b) MAPLC3 expression was detected by western blotting 24 h after indicated irradiation. Quantitative immunoblot analysis of MAPLC3 expression was represented by normalized MAPLC3-II/I ratio. (c) Immunostaining of MDC was detected by flow cytometry at 24 h after 8 Gyr irradiation. H1299 cells stably transfected with GFP-LC3 were treated with 8 Gyr irradiation and analysed by microscopy for presence of fluorescent puncta 24 h after IR. (d and e) Phosphorylation of ATM was illustrated by western blotting at 30 min, 1, 2 and 4 h after IR. Quantitative analysis was shown as the normalized ratio of P-ATM/ATM. Data are presented as mean ± SD of three independent experiments. $*P < 0.05$ versus a sham-irradiated group (mock group).

ATM or MAPK14 silenced cells. (Fig. 2e–g). The above-mentioned results suggest that apoptosis might not be the main way for ATM or MAPK14 to induce radiosensitivity.

ATM inhibition and MAPK14 blockage altered IR-induced autophagy

As the role of apoptosis has been excluded, more emphasis was laid upon the function of IR-induced autophagy on radiosensitivity, in the following study. Basal level of autophagy was different in the various groups of cells. Aiming to compare variation in IR-induced autophagy change, we took this into consideration. All changes were divided by the previous basal level, to better convey function of IR, which was represented as (after IR − before IR)/before IR. Immunofluorescence results showed that percentage of puncture-containing cells increased by 129% in DMSO-treated cells, but only increased by 47% in cells having had KU55933 treatment (Fig. 3a,b). MDC staining revealed similar outcomes, that is, IR increased autop-

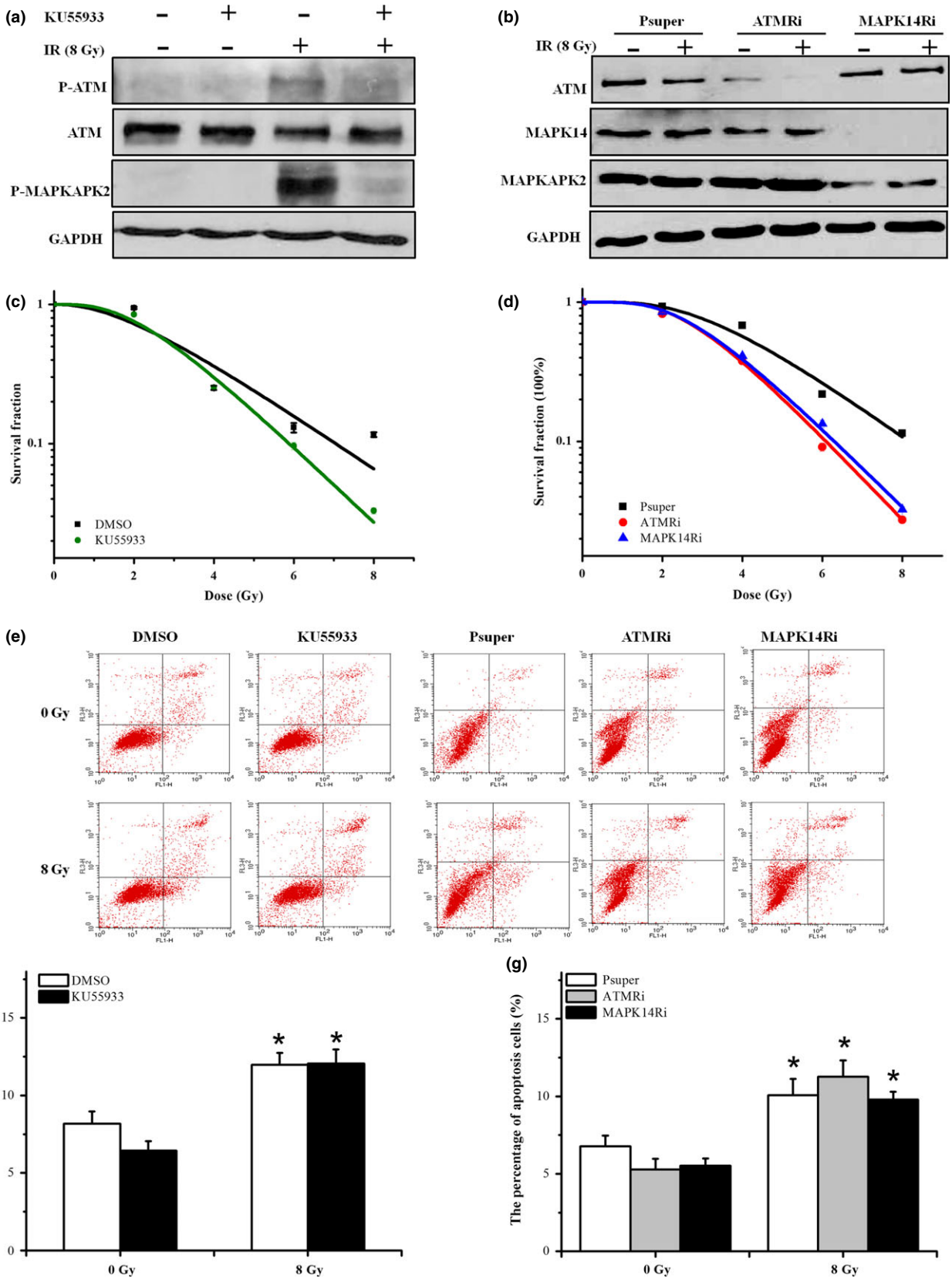

Figure 2. Inhibition of ATM increased radiation sensitivity but did not affect apoptosis. (a) H1299 cells were pre-treated with KU55933 or DMSO 2 h before IR. Western blotting was used to detect phosphorylation of ATM, total ATM and phosphorylation of MAPKAPK2 expression. (b) H1299 cells were stably transfected with ATM shRNA and MAPK14 shRNA. shRNA scramble vector was used as control (Psuper). Individual clones were obtained under puromycin selection. Knock-down effects were confirmed by western blotting. (c) H1299 cells were pre-treated with KU55933 2 h before radiation (0, 2, 4, 6 and 8 Gyr), and then radiation sensitivity was assessed by colony formation assay. (d) Radiation sensitivity was determined by colony formation assay in Psuper, $ATM^{-/-}$ and $MAPK14^{-/-}$ cell lines after radiation treatment (0, 2, 4, 6 and 8 Gy). (E) cells in (c) and (d) were treated with mock or IR (8 Gyr). Flow cytometry was used to detect apoptosis 24 h after radiation. Cells were stained with PI and Annexin V-FITC. Positive-stained cells were counted using FAC Scan. (f and g) Quantitative analysis of (e). Data are presented as mean ± SD of three independent experiments. $*P < 0.05$ versus non-IR group.

hagy by 231% in DMSO-treated cells and 24% KU55933-treated cells (Fig. 3c).

To further identify whether ATM or MAPK14 were required for IR-induced autophagy, we observed conversion of MAPLC3-I to MAPLC3-II in the cell model group. Ratios of MAPLC3-II/MAPLC3-I increased by 107% after IR in Psuper cells, while in $ATM^{-/-}$ cells it showed no change (Fig. 3d,e). Interestingly, after MAPK14 knock-down, this ratio rose to almost 2.29 times basal level of $MAPK14^{+/+}$cells, which was similar to that of Psuper cells with IR treatment. However, ratio of MAPLC3-II/MAPLC3-I then decreased by 72% after IR treatment. Thus, loss of either ATM or MAPK14 significantly reduced IR-induced autophagy. In the MDC-staining assay (Fig. 3f), autophagy induced by IR increased by 136% in Psuper cells, but only by 27% in $ATM^{-/-}$ cells. Surprisingly, MDC-positive $MAPK14^{-/-}$ cells went up by 129% before IR and went down by 55% after IR treatment, which was consistent with western blotting results. These together confirmed that both inhibition of ATM by either KU55933 or silencing and knock-down of MAPK14 repressed IR-induced autophagy in H1299 cells. Then the next question was 'how to regulate autophagy' and 'what is the underlying mechanism'?

ATM and MAPK14 regulated IR-induced autophagy through the mTOR pathway

It is well appreciated that mTOR serves as a master negative regulator of autophagy (32). In this study, western blotting demonstrated significant reduction in phospho-mTOR, phospho-pS6K and Akt (by 84%, 70% and 50%, respectively) after IR treatment (Fig. 4a,b). After combination treatment of KU55933 with IR, cells showed slight reduction in phospho-mTOR, phospho-pS6K expression and Akt (by 40%, 38% and 10% respectively). These results illustrate that IR caused down-regulation of mTOR signalling which could be inhibited by KU55933.

A direct role for ATM and MAPK14 in suppression of mTOR was further demonstrated in $ATM^{-/-}$, whereas $ATM^{+/+}$ cells significantly repressed mTORC1 in response to IR (Fig. S2a,b). However $MAPK14^{-/-}$ cells expressed remarkable reduction in mTOR level first then reversed to elevate after IR treatment, consistent with changes in MAPLC3. These results further demonstrate that ATM and MAPK14 regulate IR-induced autophagy *via* mTOR pathways.

ATM and MAPK14 affected the Beclin1/PI3KIII complex

Given that the Beclin1/PI3KIII complex is essential for driving autophagy, effects of ATM and MAPK14 on Beclin1/PI3KIII were observed using co-immunoprecipitation. As expected, Beclin1 bound to PI3KIII in DMSO-treated cells, and the interaction significantly increased after IR, as more PI3KIII was brought down by Beclin1 (Fig. 4c). However, this interaction did not change by IR after KU55933 pre-treatment. Furthermore, we found that Beclin1 interacted with more ATM after IR in DMSO-treated cells, while in KU55933-treated cells, the Beclin1–ATM interaction was prominently impaired in the absence of IR, but recovered to a higher level in kits presence.

The interaction of Beclin1 and MAPK14 was found to not change in Hela cells after ATM knock-down (31). To move forward a single step, interaction of Beclin1/p-MAPKAPK2 and Beclin1/MAPKAPK2 was detected by immunoprecipitation after IR treatment (Fig. 4d). The results illustrated that neither Beclin1/p-MAPKAPK2 interaction nor Beclin1/MAPKAPK2 interaction changed remarkably; however, both interactions were impaired by IR treatment in $ATM^{-/-}$ cells; while in $MAPK14^{-/-}$ cells, some changes were found. The above-mentioned results suggest that ATM might play roles in Beclin1/MAPKAPK2 interactions.

Discussion

Autophagy is thought to serve as tumour suppressor, as defective autophagy provides oncogenic stimuli or can cause malignant transformation and spontaneous tumours; on the other hand, it helps cells survive environmental and cellular stresses then causing resistance to anti-neoplastic therapy (33). This makes it promising to induce autophagic interference in cancer therapy (34).

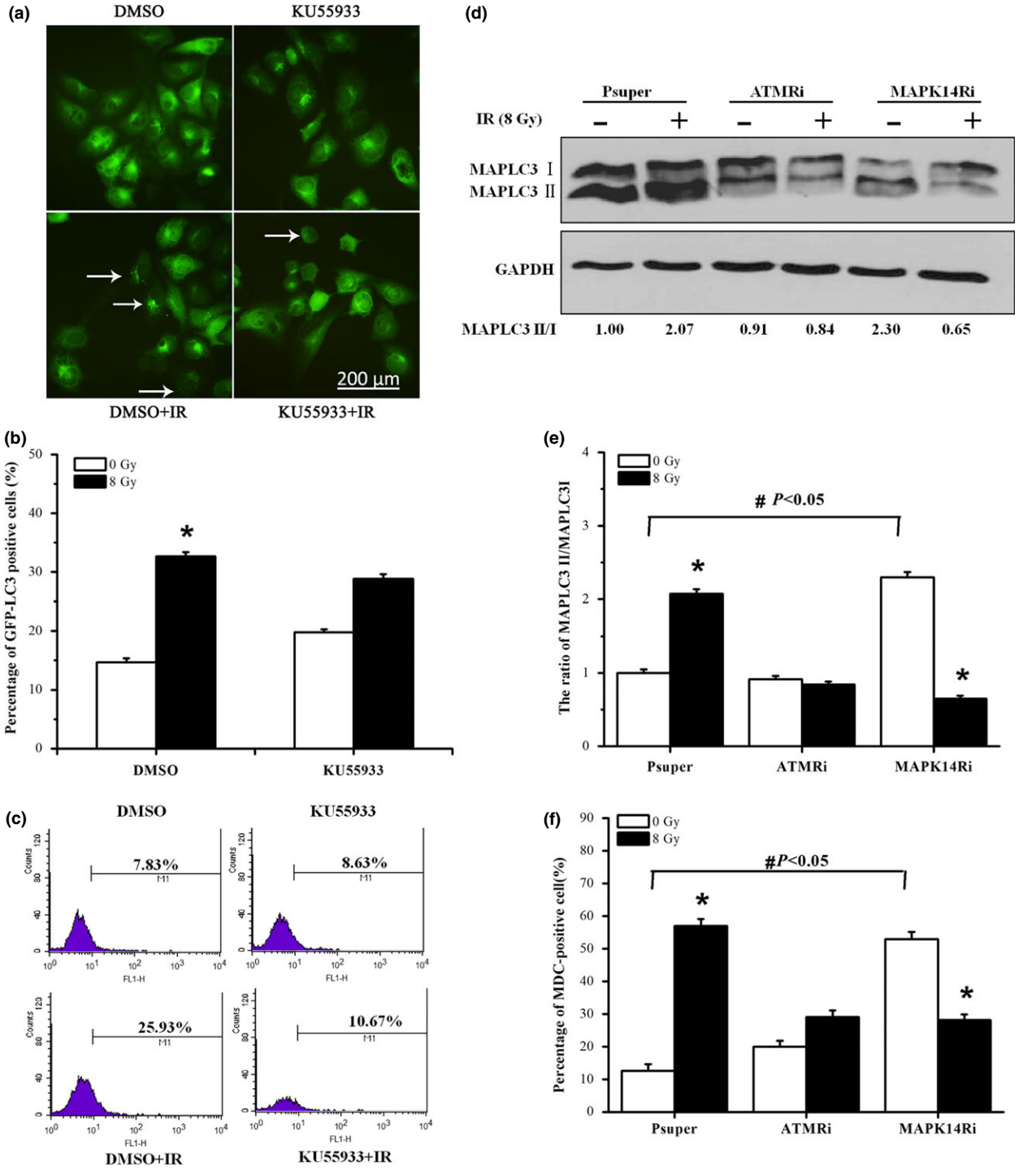

Figure 3. ATM inhibition or MAPK14 knock-down altered IR-induced autophagy. (a and b) Cells stably transfected with GFP-LC3 were pre-treated with KU55933 2 h before 8 Gy radiation then analysed using microscopy, for presence of fluorescent puncta 24 h after IR. Cells undergoing autophagy were quantified as percentage of GFP-positive cells. (c) Cells in (a) were also subjected to flow cytometry to detect MDC staining percentage 24 h after radiation. Graph shows percentage of MDC-stained cells. (d) Isogenic cell lines were treated with mock or IR (8 Gyr). Cell lysates were harvested and subjected to western blotting 24 h after radiation. (e) Quantitative analysis of (d) is shown as ratio of MAPLC3-II/MAPLC3-I, and cells transfected with Psuper used as control (100%). (f) Cells in (d) were also subjected to flow cytometry to detect MDC staining percentage 24 h after radiation. Graph shows percentage of MDC-stained cells. Data are presented as mean ± SD of three independent experiments. $^{*}P < 0.05$ versus mock group, $^{\#}P < 0.05$ versus mock group of Psuper cells.

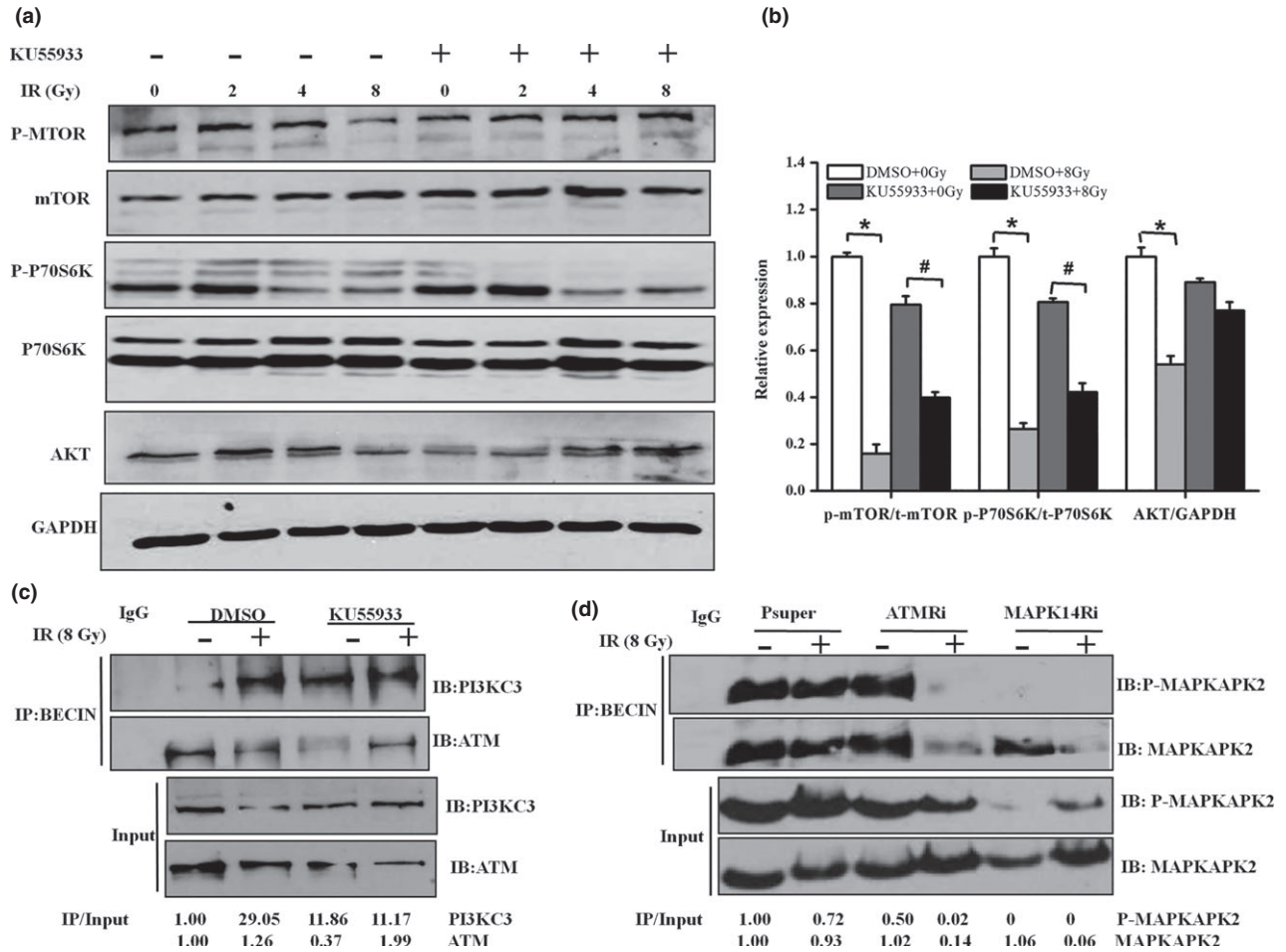

Figure 4. ATM and MAPK14 regulated the mTOR pathway and Beclin1/PI3KIII complex. (a and b) Cells pre-treated with KU55933 were exposed to radiation, and protein extracts were subjected to western blotting. Quantitative analysis is shown as ratio of p-mTOR/t-mTOR, p-p70S6K/t-p70S6K and Akt/GAPDH. Cells treated with DMSO were used as control (100%). (c) Cells were treated with mock or IR (8 Gyr) with or without KU55933 pre-treatment. Two hours after radiation, cell lysates were harvested and subjected to immunoprecipitation using Beclin1 antibody, and then blotted with indicated antibodies. (d) Isogenic cell lines were treated with mock or IR (8 Gyr). Two hours after radiation, cell lysates were harvested and subjected to immunoprecipitation using Beclin1 antibody and then blotted with indicated antibodies. Ratio of immunoprecipitation/input was normalized by cells treated with DMSO only and Psuper cells without IR treatment respectively. Data are presented as mean ± SD of three independent experiments. $^{*}P < 0.05$ versus cells treated with DMSO only, $^{\#}P < 0.05$ versus cells treated with KU55933 only.

Radiotherapy is a major strategy for cancer treatment. In this study, we found that autophagy and phosphorylation of ATM at 1981 could be induced simultaneously in H1299 lung cancer cells, by IR. However, IR-induced autophagy was inhibited by KU55933 and ATM silencing, confirming that ATM participates in this IR-induced autophagy.

MAPK14 has been reported to share the TQ263 phosphorylation motif with ATM; it is phosphorylated more than 4-fold in response to IR (21), suggesting that MAPK14 could be one of ATM's substrates. In our previous study, in Hela cells (31), expression of MAPK14 was found to be down-regulated significantly by ATM knock-down, although whether this was through transcriptional or translational regulation still needed further investigation. MAPKAPK2 is known to be directly downstream of MAPK14, whose phosphorylation represents activity of MAPK14. Aiming here to validate the role of MAPK14, MAPKAPK2 was detected to reflect the activity of MAPK14 in H1299 cells. As expected, phosphorylation of MAPKAPK2 was inhibited by KU55933, which was consistent with down-regulation of MAPK14 after ATM knock-down, and also consistent with reduction in phosphorylation of ATM. This confirmed that MAPK14 is indeed, one of the substrates of ATM and thus is regulated by ATM.

To understand the functions of these molecules, effects of ATM and MAPK14 on radiosensitivity were detected. Both KU55933 treatment and ATM silencing

led to hypersensitivity in H1299 cells. Interestingly, MAPK14$^{-/-}$ cells had a similar sensitivity to IR with ATM$^{-/-}$ cells, suggesting MAPK14 might be the main downstream molecule of ATM, to regulate cell death. As we known, apoptosis and autophagy are the most important mechanisms of cell death; we then aimed to discover which of them would function in this process. In contrast to Eun's study (35), we found that neither ATM knock-down nor MAPK14 knock-down influenced IR-induced apoptosis compared to Psuper cells, which might be due to different sources and/or different types of irradiation (X-rays versus γ-rays; 8 Gy versus 10 Gy; complete apoptosis versus early apoptosis). It has been suggested that excessive induction of autophagy canl turn into programmed cell death mechanisms when cell damage is beyond repair limitation (36). Thus, we hypothesized that IR-induced autophagy might be the underlying mechanism of hypersensitivity resulting from ATM or MAPK14 knock-down. The role of ATM in regulating autophagy has been recently reported. When exposed to genotoxic and oxidative stresses such as IR, ROS or NO, ATM is rapidly activated, which in turn stimulates the LKB1/AMPK/TSC2 signalling pathway and results in repression of mTORC1 activity, thereby inducing autophagy (18,19,37). Up to now, the relationship between MAPK14 and autophagy, but not IR-induced autophagy, has been studied (25,26,38,39) and MAPK14 has been proven to play a dual role in it, as both positive and negative regulator. As the possible downstream substrate of ATM, we wondered whether ATM could regulate MAPK14 and consequently affect autophagic processes induced by IR. Aiming to compare variations in autophagic changes, we took its basal level into consideration. As expected, our observations indicated that KU55933 inhibited IR-induced autophagy from 129% to 47%, and ATM knock-down by itself blocked conversion of MAPLC3-I to MAPLC3-II after IR. IR-induced autophagy was absent in ATM$^{-/-}$cells, suggesting that ATM was required for IR-induced autophagy, which was consistent with observations in Hela cells (31). However, there is an obvious difference between H1299 and Hela cells. Knock-down of MAPK14 itself up-regulates basal autophagy in H1299 cells but not in Hela cells, which might result from partial deletion of p53 in H1299 cells. There could be three possible reasons for the above phenomenon: first, direct competition of MAPK14 with mAtg9 for binding to p38IP gives rise to trafficking of autophagy (24,40); secondly, MAPK14-driven metabolic reprogramming cannot sustain production of NADPH, resulting in increased levels of ROS (41,42); thirdly, MAPK14-mediated p53 phosphorylation suppresses its ubiquitination then increases p53 protein stability in p53 partially deleted H1299 cells, resulting in p53-DRAM1-induced autophagy (30,43). Evidence of the above makes it possible that MAPK14 deficiency can lead to increased autophagy. As for the prominent reduction of IR-induced autophagy, it can be easily understood. Induction of autophagy by PGF, IFN-γ and SN38 and some other stimulators are all dependent on MAPK14 activation (28,30,44). But the role of MAPK14 in IR-induced autophagy was first studied in our work. In conclusion, the MAPK14 pathway activation as well as ATM was necessary for occurrence of autophagy induced by IR in H1299 cells.

Together with our previous work, we have confirmed that ATM regulated IR-induced autophagy through the MAPK14 pathway, in human cervical cancer Hela cells and human lung cancer H1299 cells. Given that MAPK14 and ATM were required for autophagy induced by IR in H1299, we turned to the mechanism of how ATM regulated MAPK14 and consequently triggered IR-induced autophagy.

It has been reported that ATM stimulates the mTOR pathway through the LBK/AMPK/TSC2 pathway, which in turn results in mTORC1 repression and induction of autophagy (16,37). Here MAPK14 acted as a negative upstream signal regulating autophagy in an mTOR-dependent manner (37,38) and the mTOR pathway also can be regulated by the ERK1/2 and MAPK signalling pathway (45). According to our observations, repression of mTORC1 in response to IR and phosphorylation of P70S6K by mTOR were not observed after ATM and MAPK14 silencing, while down-regulation of the mTOR pathway was partly reversed by KU55933, which is consistent with the change of IR-induced autophagy. As a result, we conclude that ATM and MAPK14 regulate IR-induced autophagy partially *via* repression of the mTOR pathway. Beclin1/PI3KIII complexes were considered to participate in distinct steps of autophagy regulation, either at the early stages to promote autophagosome formation or at later ones to promote autophagosome maturation (46). Anti-apoptotic protein Bcl2 binding to Beclin1 inhibits Beclin1 activity and consequently suppresses autophagy in yeast and mammalian cells (47). We identified that the Beclin1–PI3KIII interaction was enhanced in response to DNA damage induced by IR, which is inhibited by KU55933, resulting in abolishion of IR-induced autophagy. ATM has been reported to interact with Beclin1 and to phosphorylate Beclin1 at Thr57, resulting in dissociation of the Beclin l/Bcl-2 complex. In this research, we also found that ATM interacted with Beclin1, resulting in dissociation of Beclin1 from the Beclin1/Bcl-2 complex, which consequently triggered autophagy. Taken together, inhibition of ATM impaired formation of the

Beclin1/PI3KIII complex, which is necessary for autophagy.

Finally but most importantly, we found the interaction MAPK14–Beclin1 could be regulated by ATM (31). To further identify this mechanism, the interaction between Beclin 1 and MAPKAPK2 was further assessed after immunoprecipitation. Neither the Beclin1/p-MAPKAPK2 interaction nor that of Beclin1/MAPKAPK2 was clearly changed; however, both interactions were impaired by IR treatment in $ATM^{-/-}$ cells. In other words, both the interaction Beclin1/MAPKAPK2 and the interaction of Beclin1/MAPK14 were regulated by ATM, which indicated that ATM regulated Beclin/PI3KIII complexes through the MAPK14 pathway. Apart from the well-characterized ATR/CHK1 and ATM/CHK2 pathways, MAPK14 and MAPKAPK2 have recently been considered to be the third effector kinase complex to block cell cycle progression in response to DNA damage (48,49). MAPKAPK2 has been shown to share substrate homology with both Chk1 and Chk2. MAPKAPK2 has been reported to phosphorylate ATDC at Ser-550 in an ATM-dependent manner, resulting in radioprotection (50), which is considered to be more important. Thus, we deduced that MAPKAPK2 might have an effect on Beclin1/PI3KIII complexes. Accordingly, we found that the ATM/MAPK14/MK2 checkpoint functioned as a prominent role in response to DNA damage, which contributed to the connection of IR-induced cell cycle and autophagy together. The exact mechanism of this still needs further study.

In summary, autophagy and phosphorylation of ATM at 1981 was induced by IR in H1299 cells. MAPK14, as one of substrates of ATM, was found to be directly regulated by ATM, which affected IR-induced autophagy through the mTOR signalling pathway and the Beclin1/PI3KIII complex, consequently contributing to hypersensitivity.

Acknowledgements

We thank Glenda Kannwischer for the revision of this manuscript. The study was supported by NSFC grant (30770649, 30970682, 31370837), Research Fund for the Doctoral Program of Higher Education of China (20100061110070), Program for New Century Excellent Talents in University, the Fundamental Research Funds for the Jilin University.

Conflict of interest

The authors declare that they have no conflicting interests.

References

1 Nguyen NP, Bishop M, Borok TJ, Welsh J, Hamilton R, Cohen D *et al.* (2010) Pattern of failure following chemoradiation for locally advanced non-small cell lung cancer: potential role for stereotactic body radiotherapy. *Anticancer Res.* **30**, 953–961.
2 Tyldesley S, Boyd C, Schulze K, Walker H, Mackillop WJ (2001) Estimating the need for radiotherapy for lung cancer: an evidence-based, epidemiologic approach. *Int. J. Radiat. Oncol. Biol. Phys.* **49**, 973–985.
3 Levine B, Kroemer G (2008) Autophagy in the pathogenesis of disease. *Cell* **132**, 27–42.
4 Sahu R, Kaushik S, Clement CC, Cannizzo ES, Scharf B, Follenzi A *et al.* (2011) Microautophagy of cytosolic proteins by late endosomes. *Dev. Cell* **20**, 131–139.
5 Li W, Yang Q, Mao Z (2011) Chaperone-mediated autophagy: machinery, regulation and biological consequences. *Cell. Mol. Life Sci.* **68**, 749–763.
6 Kroemer G, Marino G, Levine B (2010) Autophagy and the integrated stress response. *Mol. Cell* **40**, 280–293.
7 Mizushima N (2007) Autophagy: process and function. *Genes Dev.* **21**, 2861–2873.
8 Shintani T, Klionsky DJ (2004) Autophagy in health and disease: a double-edged sword. *Science* **306**, 990–995.
9 Townsend KN, Hughson LR, Schlie K, Poon VI, Westerback A, Lum JJ (2012) Autophagy inhibition in cancer therapy: metabolic considerations for antitumor immunity. *Immunol. Rev.* **249**, 176–194.
10 White E (2012) Deconvoluting the context-dependent role for autophagy in cancer. *Nat. Rev. Cancer* **12**, 401–410.
11 Wu WK, Coffelt SB, Cho CH, Wang XJ, Lee CW, Chan FK *et al.* (2012) The autophagic paradox in cancer therapy. *Oncogene* **31**, 939–953.
12 Tanida I (2011) Autophagosome formation and molecular mechanism of autophagy. *Antioxid. Redox Signal.* **14**, 2201–2214.
13 Gutierrez MG, Master SS, Singh SB, Taylor GA, Colombo MI, Deretic V (2004) Autophagy is a defense mechanism inhibiting BCG and Mycobacterium tuberculosis survival in infected macrophages. *Cell* **119**, 753–766.
14 Wang CW, Klionsky DJ (2003) The molecular mechanism of autophagy. *Mol. Med.* **9**, 65–76.
15 Sapkota GP, Deak M, Kieloch A, Morrice N, Goodarzi AA, Smythe C *et al.* (2002) Ionizing radiation induces ataxia telangiectasia mutated kinase (ATM)-mediated phosphorylation of LKB1/STK11 at Thr-366. *Biochem. J.* **368**, 507–516.
16 Alexander A, Walker CL (2011) The role of LKB1 and AMPK in cellular responses to stress and damage. *FEBS Lett.* **585**, 952–957.
17 Alexander A, Cai SL, Kim J, Nanez A, Sahin M, MacLean KH *et al.* (2010) ATM signals to TSC2 in the cytoplasm to regulate mTORC1 in response to ROS. *Proc. Natl Acad. Sci. USA* **107**, 4153–4158.
18 Menendez JA, Cufi S, Oliveras-Ferraros C, Martin-Castillo B, Joven J, Vellon L *et al.* (2011) Metformin and the ATM DNA damage response (DDR): accelerating the onset of stress-induced senescence to boost protection against cancer. *Aging (Albany NY)* **3**, 1063–1077.
19 Singh K, Matsuyama S, Drazba JA, Almasan A (2012) Autophagy-dependent senescence in response to DNA damage and chronic apoptotic stress. *Autophagy* **8**, 236–251.
20 Chen LH, Loong CC, Su TL, Lee YJ, Chu PM, Tsai ML *et al.* (2011) Autophagy inhibition enhances apoptosis triggered by BO-1051, an N-mustard derivative, and involves the ATM signaling pathway. *Biochem. Pharmacol.* **81**, 594–605.

21 Matsuoka S, Ballif BA, Smogorzewska A, McDonald ER 3rd, Hurov KE, Luo J *et al.* (2007) ATM and ATR substrate analysis reveals extensive protein networks responsive to DNA damage. *Science* **316**, 1160–1166.
22 Wagner EF, Nebreda AR (2009) Signal integration by JNK and p38 MAPK pathways in cancer development. *Nat. Rev. Cancer* **9**, 537–549.
23 Chiacchiera F, Simone C (2008) Signal-dependent regulation of gene expression as a target for cancer treatment: inhibiting p38alpha in colorectal tumors. *Cancer Lett.* **265**, 16–26.
24 Webber JL (2010) Regulation of autophagy by p38alpha MAPK. *Autophagy* **6**, 292–293.
25 Chiacchiera F, Matrone A, Ferrari E, Ingravallo G, Lo Sasso G, Murzilli S *et al.* (2009) p38alpha blockade inhibits colorectal cancer growth in vivo by inducing a switch from HIF1alpha- to FoxO-dependent transcription. *Cell Death Differ.* **16**, 1203–1214.
26 Chiacchiera F, Simone C (2009) Inhibition of p38alpha unveils an AMPK-FoxO3A axis linking autophagy to cancer-specific metabolism. *Autophagy* **5**, 1030–1033.
27 Chiacchiera F, Grossi V, Cappellari M, Peserico A, Simonatto M, Germani A *et al.* (2012) Blocking p38/ERK crosstalk affects colorectal cancer growth by inducing apoptosis in vitro and in preclinical mouse models. *Cancer Lett.* **324**, 98–108.
28 Hou HH, Cheng SL, Chung KP, Kuo MY, Yeh CC, Chang BE *et al.* (2014) Elastase induces lung epithelial cell autophagy through placental growth factor: a new insight of emphysema pathogenesis. *Autophagy* **10**, 1509–1521.
29 Zhong W, Zhu H, Sheng F, Tian Y, Zhou J, Chen Y *et al.* (2014) Activation of the MAPK11/12/13/14 (p38 MAPK) pathway regulates the transcription of autophagy genes in response to oxidative stress induced by a novel copper complex in HeLa cells. *Autophagy* **10**, 1285–1300.
30 Paillas S, Causse A, Marzi L, de Medina P, Poirot M, Denis V *et al.* (2012) MAPK14/p38alpha confers irinotecan resistance to TP53-defective cells by inducing survival autophagy. *Autophagy* **8**, 1098–1112.
31 Liang N, Jia L, Liu Y, Liang B, Kong D, Yan M *et al.* (2013) ATM pathway is essential for ionizing radiation-induced autophagy. *Cell. Signal.* **25**, 2530–2539.
32 Codogno P, Meijer AJ (2005) Autophagy and signaling: their role in cell survival and cell death. *Cell Death Differ.* **12**(Suppl 2), 1509–1518.
33 Dalby KN, Tekedereli I, Lopez-Berestein G, Ozpolat B (2010) Targeting the prodeath and prosurvival functions of autophagy as novel therapeutic strategies in cancer. *Autophagy* **6**, 322–329.
34 Liu H, He Z, Simon HU (2013) Targeting autophagy as a potential therapeutic approach for melanoma therapy. *Semin. Cancer Biol.* **23**, 352–360.
35 Cho EA, Kim EJ, Kwak SJ, Juhnn YS (2014) cAMP signaling inhibits radiation-induced ATM phosphorylation leading to the augmentation of apoptosis in human lung cancer cells. *Mol. Cancer.* **13**, 36.
36 Chen Y, Klionsky DJ (2011) The regulation of autophagy – unanswered questions. *J. Cell Sci.* **124**, 161–170.
37 Tripathi DN, Chowdhury R, Trudel LJ, Tee AR, Slack RS, Walker CL *et al.* (2013) Reactive nitrogen species regulate autophagy through ATM-AMPK-TSC2-mediated suppression of mTORC1. *Proc. Natl Acad. Sci. USA* **110**, E2950–E2957.
38 Tang G, Yue Z, Talloczy Z, Hagemann T, Cho W, Messing A *et al.* (2008) Autophagy induced by Alexander disease-mutant GFAP accumulation is regulated by p38/MAPK and mTOR signaling pathways. *Hum. Mol. Genet.* **17**, 1540–1555.
39 Luo Y, Zou P, Zou J, Wang J, Zhou D, Liu L (2011) Autophagy regulates ROS-induced cellular senescence via p21 in a p38 MAPKalpha dependent manner. *Exp. Gerontol.* **46**, 860–867.
40 Webber JL, Tooze SA (2010) Coordinated regulation of autophagy by p38alpha MAPK through mAtg9 and p38IP. *EMBO J.* **29**, 27–40.
41 Comes F, Matrone A, Lastella P, Nico B, Susca FC, Bagnulo R *et al.* (2007) A novel cell type-specific role of p38alpha in the control of autophagy and cell death in colorectal cancer cells. *Cell Death Differ.* **14**, 693–702.
42 Desideri E, Vegliante R, Cardaci S, Nepravishta R, Paci M, Ciriolo MR (2014) MAPK14/p38alpha-dependent modulation of glucose metabolism affects ROS levels and autophagy during starvation. *Autophagy* **10**, 1652–1665.
43 Xie X, Le L, Fan Y, Lv L, Zhang J (2012) Autophagy is induced through the ROS-TP53-DRAM1 pathway in response to mitochondrial protein synthesis inhibition. *Autophagy* **8**, 1071–1084.
44 Matsuzawa T, Fujiwara E, Washi Y (2014) Autophagy activation by interferon-gamma via the p38 mitogen-activated protein kinase signalling pathway is involved in macrophage bactericidal activity. *Immunology* **141**, 61–69.
45 Sun Y, Zou M, Hu C, Qin Y, Song X, Lu N *et al.* (2013) Wogonoside induces autophagy in MDA-MB-231 cells by regulating MAPK-mTOR pathway. *Food Chem. Toxicol.* **51**, 53–60.
46 Qased AB, Yi H, Liang N, Ma S, Qiao S, Liu X (2013) MicroRNA-18a upregulates autophagy and ataxia telangiectasia mutated gene expression in HCT116 colon cancer cells. *Mol. Med. Rep.* **7**, 559–564.
47 Pattingre S, Tassa A, Qu X, Garuti R, Liang XH, Mizushima N *et al.* (2005) Bcl-2 antiapoptotic proteins inhibit Beclin 1-dependent autophagy. *Cell* **122**, 927–939.
48 Reinhardt HC, Yaffe MB (2009) Kinases that control the cell cycle in response to DNA damage: Chk1, Chk2, and MK2. *Curr. Opin. Cell Biol.* **21**, 245–255.
49 Cannell IG, Kong YW, Johnston SJ, Chen ML, Collins HM, Dobbyn HC *et al.* (2010) p38 MAPK/MK2-mediated induction of miR-34c following DNA damage prevents Myc-dependent DNA replication. *Proc. Natl Acad. Sci. USA* **107**, 5375–5380.
50 Wang L, Yang H, Palmbos PL, Ney G, Detzler TA, Coleman D *et al.* (2014) ATDC/TRIM29 phosphorylation by ATM/MAPKAP kinase 2 mediates radioresistance in pancreatic cancer cells. *Cancer Res.* **74**, 1778–1788.

Supporting Information

Additional Supporting Information may be found in the online version of this article:

Fig. S1 Cell viability of H1299 detected after KU55933 treatment. H1299 cells were exposed to indicated concentrations of KU55933, DMSO being used as control. Cell viability was analysed by CCK-8 assay. Data were presented as mean ± SD of three independent experiments. $*P < 0.05$ versus DMSO group.

Fig. S2 ATM and MAPK14 regulated the mTOR pathway in knock-down cells. Isogenic cell lines were treated with mock or IR (8 Gyr). Cell lysates were harvested 24 h after radiation and subjected to western blotting. Quantitative analysis was shown to be the ratio of mTOR/GAPDH, and Psuper cells treated with mock were used as control (100%). Data are presented as mean ± SD of three independent experiments. $*P < 0.05$ versus control group.